

PAPER • OPEN ACCESS

Melting curve of Si by means of the Z-method

To cite this article: Felipe González-Cataldo *et al* 2018 *J. Phys.: Conf. Ser.* **1043** 012038

View the [article online](#) for updates and enhancements.

Related content

- [The Melting Curve of Solid \$^3\text{He}\$ in High Magnetic Fields](#)
C. C. Kranenburg, S. A. J. Wieggers, P. G. van der Haar *et al.*
- [Fluid–fluid–solid triple point on melting curves at high temperatures](#)
G E Norman and I M Saitov
- [Z method calculations to determine the melting curve of silica at high pressures](#)
F. González-Cataldo, S. Davis and G. Gutiérrez



IOP | ebooks™

Bringing you innovative digital publishing with leading voices to create your essential collection of books in STEM research.

Start exploring the collection - download the first chapter of every title for free.

Melting curve of Si by means of the Z-method

Felipe González-Cataldo¹, Fernando Corvacho², Gonzalo Gutiérrez²

¹Department of Earth and Planetary Science, University of California, Berkeley, California 94720, USA.

²Grupo de NanoMateriales, Departamento de Física, Facultad de Ciencias, Universidad de Chile, Casilla 653, Santiago, Chile

E-mail: f_gonzalez@berkeley.edu

Abstract. The melting curve of silicon is investigated through classical molecular dynamics simulations. We explore pressures from 0 to 20 GPa using the EDIP, Stillinger-Weber, and Tersoff interatomic potentials. Using the Z method, we demonstrate that the predicted melting temperature T_m can be significantly overestimated, depending on the potential chosen. Our results show that none of the potentials explored is able to reproduce the experimental melting curve of silicon by means of the Z-method. However, the EDIP potential does predict the change in the Clapeyron slope, associated with the diamond to β -tin phase transition.

1. Introducción

Solid silicon is a key material in the semiconductor industry, and has played a major role in the development of new technologies. At ambient pressure, Si crystallizes in the diamond structure, and transforms to the metallic β -tin structure around 12 GPa. Many aspects of the phase diagram of Si have been studied, such as the identification of different structures up to 250 GPa [1, 2], but an accurate determination of the melting curve still remains challenging, since high-temperature and high-pressure experiments on Si are difficult. Therefore, the available data need further theoretical confirmation.

The Z method is a novel technique that allows to determine the melting temperature of a material, based on a series of simulations at constant volume. The method has been applied to study wide variety of materials, such as Ar [3], Ta [4], Pt [5], SiO₂ [6], BeO [7], and many others, showing good agreement with other methods, and experiments. In this paper, we explore the predictions of the Z method for Si when different empirical potentials are used in classical molecular dynamics.

2. Methodology

2.1. Classical Molecular Dynamics

Since its development in 1960, Molecular Dynamics (MD) has been a powerful tool to study the properties of materials from their atoms interactions. Given an empirical interatomic potential, macroscopic properties of a material can be calculated by integrating the equations of motion of the atoms in the system and applying the theorems from Statistical Mechanics [8]. Nowadays, many softwares are available to perform MD, being LAMMPS [9] one of the most widely used. LAMMPS comes with several empirical potentials available, including the Tersoff [10, 11], EDIP [12], and Stillinger-Weber (SW) potentials [13], whose parameters have been adjusted



from ab initio simulations and have shown to properly describe the mechanical properties of silicon.

The SW potential has been shown to reproduce the pair-correlation function $g(r)$ of the liquid, and was fit to reproduce the melting temperature T_m at ambient pressure to within a few hundred degrees of the experimental value of 1685 K [13]. The Tersoff potentials have been widely used to study silicon, but it is well known that it has problems describing the elastic constants and melting point. On the other hand, a modified version of Tersoff, so called MOD [14], shows good agreement with the experimental value of the melting temperature at ambient pressure. EDIP is an empirical potential that is also an improvement to the Tersoff potentials and, although it was developed earlier than MOD, it also reproduces the melting point of Si at ambient pressure, together with an accurate description of several structural properties. (Details about their functional form can be found in Appendix A). Thus, it is our purpose to benchmark the Z method for Si with all these potentials to show the differences in the prediction of the melting temperature for different pressures.

Using a cubic cell of 8000 atoms in the diamond structure, we carried out simulations of Si in the microcanonical ensemble for several densities, from 2.12 to 2.98 g/cm³. We used a time step of $\Delta t = 1$ fs, and a simulation time of at least 50 ps to converge the thermodynamic properties.

2.2. Z Method

The Z method is a procedure that has been extensively used in multiple melting studies, even in materials with anomalous melting curves, such as Li [15] and H [16]. The idea is to perform ab initio or classical MD in the microcanonical ensemble (NVE) on a single solid system at different initial total energies. The total energy is controlled by setting a different initial temperature in each simulation. When the crystal is heated beyond its overheating limit, the temperature naturally drops to the melting temperature as the latent heat is removed from the kinetic energy (see Figure 1). The connected P–T points on the isochore form a Z-shaped curve. Several simulations for each isochore are needed in order to yield an accurate melting temperature.

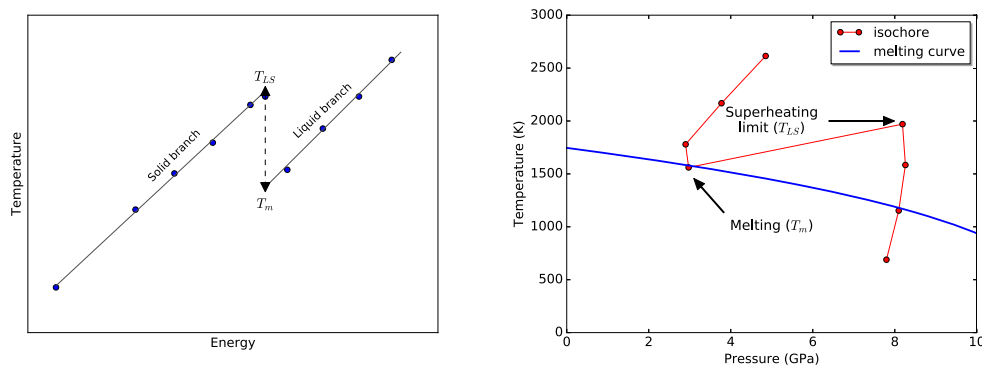


Figure 1. Schematic representation of the isochoric lines in Z-method simulations. T_{LS} is the maximum overheating temperature, and T_m the melting temperature.

2.3. Mean Squared Displacement

The Mean Squared Displacement (MSD) is a measure of the average displacement of atoms in a given sample, given by

$$\langle r^2(\tau) \rangle = \langle (\vec{r}_i(t_0 + \tau)^2 - \vec{r}_i(t_0))^2 \rangle_{t_0, i}, \quad (1)$$

where the average is taken over all particles i and time spans t_0 . For the Z method, it allows to discriminate a solid from the liquid. When the atoms oscillate around the lattice positions, the slope of MSD is zero, meaning that the material is solid. If the MSD has a positive slope, the material is liquid. We calculated the MSD using the LPMD software [17], which allows to perform and analyze molecular dynamics simulations from different formats. In Figure 2 we show the MSD of Si for different temperatures along an isochore.

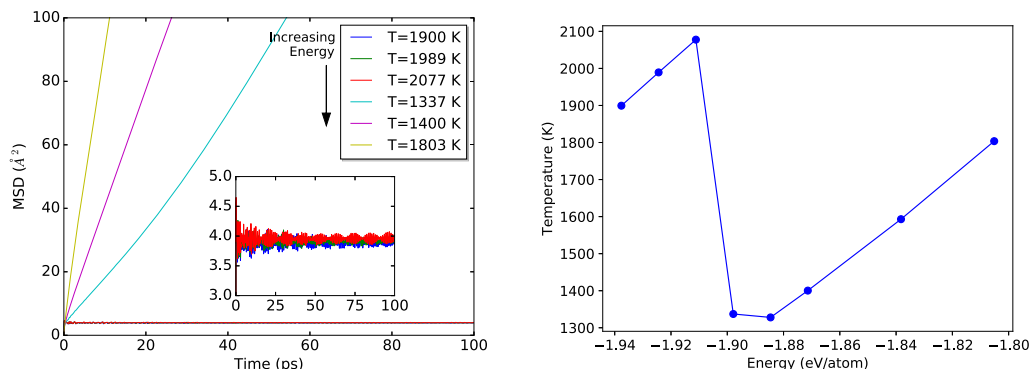


Figure 2. MSD for Si at a density $\rho = 2.515 \text{ g/cm}^3$. The system melts when its initial temperature is $T_0 = 4600 \text{ K}$, which drops to a melting temperature of 1337 K for this density. The pressure equilibrates to 1.74 GPa after melting.

When we initialized the system at $T_0 = 4600 \text{ K}$, it reached an equilibrium temperature of $T = 2077 \text{ K}$ still in solid state. When the energy was increased, the equilibrium temperature drops to a melting temperature of 1337 K . In the simulations that were close to the melting temperature, we observed that a long time was needed to completely melt the sample. Instabilities in the overheated diamond structure (Figure 3(a)) give rise to nucleation zones (Figure 3(b)), which grow until they completely melt the crystal (Figure 3(c) and 3(d)). We used OVITO [18] to identify the atoms that are coordinated in the diamond structure, and separate them from the liquid (red atoms in Figure 3).

3. Z method for different potentials

In Figures 4 and 5 we show different isochores Si using the EDIP and SW potentials. To reduce the size effects, for each isochore, we repeated all the simulations close to the melting point using 16000 atoms, and a relaxation time of 200 ps to ensure convergence.

We observe that, regardless of the potential used, the shape of the Z curve is inverted, as it has been observed in the case of lithium [15]. This is a clear signature of materials with negative Clausius-Clapeyron slope. We also notice that the variation in pressure between the overheated solid and the liquid is sometimes higher than 20 GPa, specially for Tersoff potentials. Each isochore varies significantly depending on the potential used. That has serious consequences on the prediction of the specific heat $C_v = (\partial U / \partial T)_V$, which is precisely the shape of the Z curve in the $E-T$ phase space. On Figure 6 we show all the melting temperatures in the diagrams above, each one corresponding to a different isochore.

We observe that, consistent with previous results, the Tersoff potential T3 significantly overestimates the melting temperature of Si (around 20% higher than the melting temperatures reported by Deb). However, the MOD potential significantly underestimates the melting temperatures, despite the fact that it is an improvement to T3 and that it does reproduce

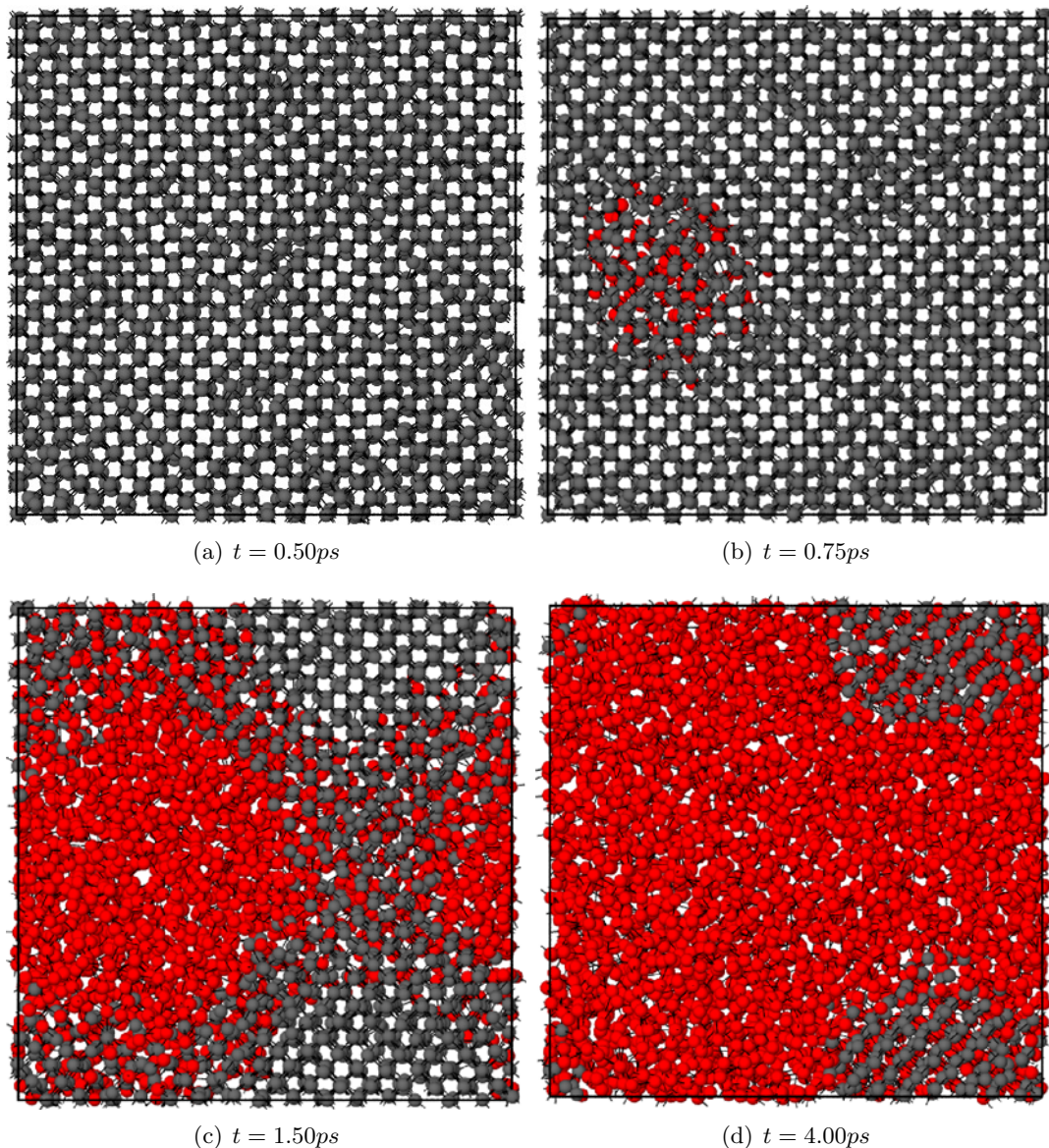


Figure 3. Melting of an overheated Si crystal during a simulation for the density $\rho = 2.515$ g/cm³. Red atoms represent the liquid, while gray atoms remain in diamond coordination. Small crystals remain solid for long periods of time in the simulation, but melt later on. The pressure equilibrates at 7.2 GPa, and the temperature drops from the initial $T_0 = 4600$ K to $T_m = 1337$ K.

the melting temperature at zero pressure. We conclude that Tersoff potentials are not suited to simulate melting processes in any of its forms, using the Z method.

On the other hand, EDIP predicts a melting temperature of $T_m = 1500$ K at zero pressure that, although it is similar to the one predicted by MOD, is more than 100 K below the experimental melting temperature. It is interesting to notice that EDIP predicts a melting curve that changes slope around 7 GPa. Although it is far from the β -tin transition that occurs at 12 GPa, it is a signature of a solid-solid phase transition occurring below the melting curve. The SW potential predicts significantly high melting temperatures at high pressures. It also predicts a positive Clapeyron slope, regardless of the pressure range. However, it seems to agree

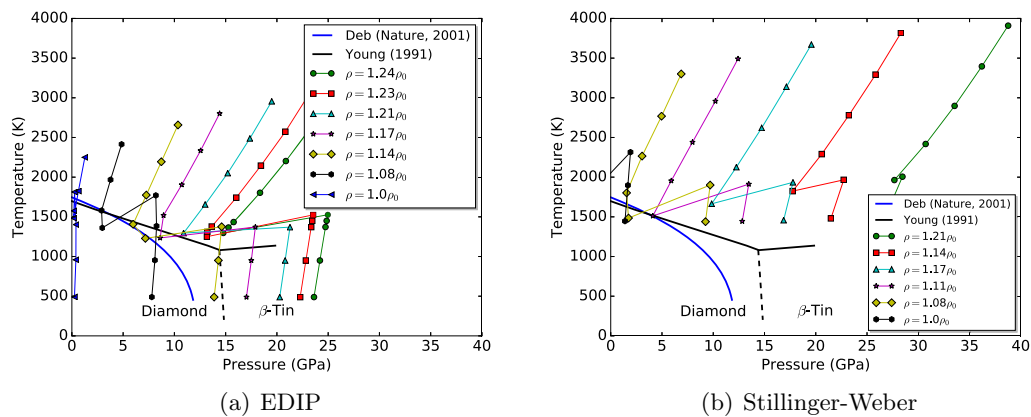


Figure 4. Silicon isochores obtained with the EDIP and SW potentials. The experimental melting curve of Si from Deb [19] and Young [20] are shown as reference. $\rho_0 = 2.33 \text{ g/cm}^3$.

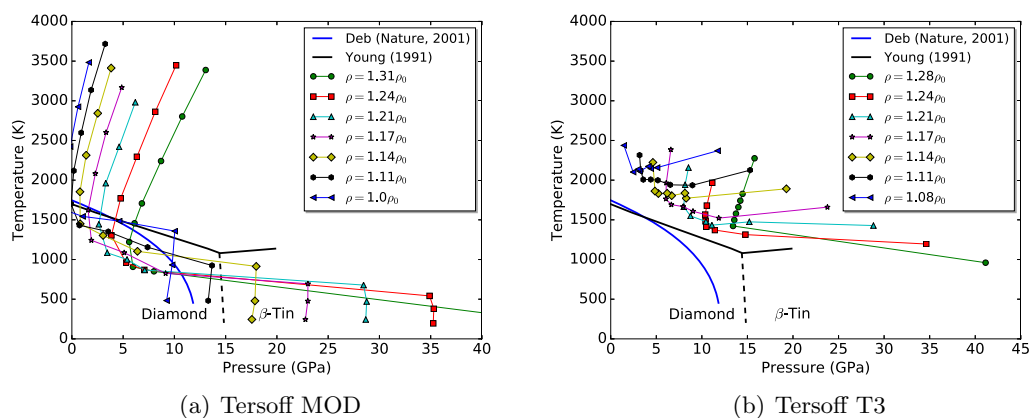


Figure 5. Silicon isochores obtained with the MOD and T3 potentials. The experimental melting curve of Si from Deb [19] and Young [20] are shown as reference. $\rho_0 = 2.33 \text{ g/cm}^3$.

with the predictions from EDIP and MOD. Nevertheless, using the Z method, the SW is not capable of reproducing the 1685 K for the ambient pressure melting temperature.

Further research is needed regarding the use of Z method with classical potentials for Si. Improvements to the Z method, such as the inverse Z methodology [5], the two phase method [21], and first principles molecular dynamics must be considered to explain the mismatch on the predictions of the melting temperature of Si.

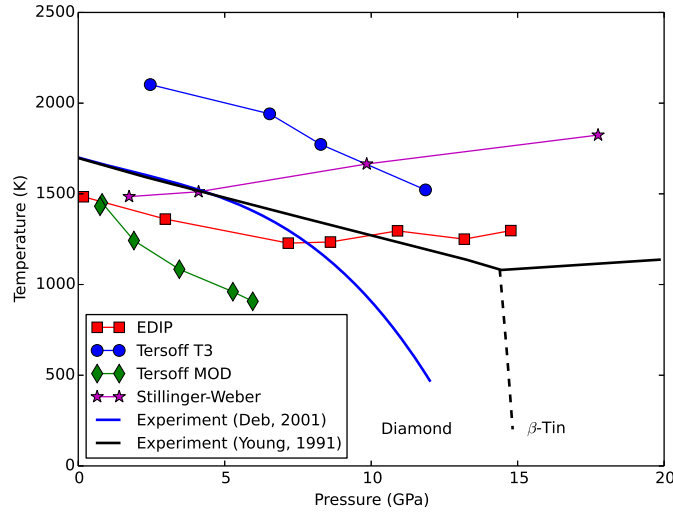


Figure 6. Melting points of Si obtained from the different interatomic potentials. The experimental melting curve of Si from Deb [19] and Young [20] are shown as reference.

Appendix A. Functional form of the potentials

The functional form of the EDIP potential is given by

$$E_i = \sum_{j \neq i} \phi_2(R_{ij}, Z_i) + \sum_{j \neq i} \sum_{k \neq i, k > j} \phi_3(R_{ij}, R_{ik}, Z_i) \quad (\text{A.1})$$

where

$$\phi_2(r, Z) = A \left[\left(\frac{B}{r} \right)^\rho - e^{-\beta Z^2} \right] \exp \left(\frac{\sigma}{r-a} \right), \quad (\text{A.2})$$

$$\phi_3(R_{ij}, R_{ik}, Z_i) = \exp \left(\frac{\gamma}{R_{ij}-a} \right) \exp \left(\frac{\gamma}{R_{ik}-a} \right) h(\cos(\theta_{ijk}), Z_i), \quad (\text{A.3})$$

$$Z_i = \sum_{m \neq i} f(R_{im}) \quad (\text{A.4})$$

$$f(r) = \begin{cases} 1 & r < c \\ \exp \left(\frac{\alpha}{1 - \left(\frac{r-c}{a-c} \right)^{-3}} \right) & c < r < a \\ 0 & r > a \end{cases}, \quad (\text{A.5})$$

$$h(l, Z) = \lambda \left[(1 - e^{-Q(Z)(l+\tau(Z))^2}) + \eta Q(Z)(l + \tau(Z))^2 \right], \quad (\text{A.6})$$

$$Q(Z) = Q_0 e^{-\mu Z} \quad (\text{A.7})$$

$$\tau(Z) = u_1 + u_2 (u_3 e^{-u_4 Z} - e^{-2u_4 Z}) \quad (\text{A.8})$$

For a given configuration of atomic positions $\{R_i\}$, the energy over the atom i is given by E_i , where ϕ_2 represents the pair potential part, and ϕ_3 the three-body interactions. The effective coordination number, Z_i , is given as a sum of $f(R_{im})$, which represents the contribution of the m closest neighbors.

$A = 7.9821730$ [eV]	$Q_o = 312.1341346$
$B = 1.5075463$ [Å]	$\mu = 0.6966326$
$a = 3.1213820$ [Å]	$\beta = 0.0070975$
$c = 2.5609104$ [Å]	$\alpha = 3.1083847$
$\sigma = 0.5774108$ [Å]	$u_1 = -0.165799$
$\lambda = 1.4533108$ [eV]	$u_2 = 32.557$
$\gamma = 1.1247945$ [Å]	$u_3 = 0.286198$
$\rho = 1.2085196$	$u_4 = 0.66$
$\eta = 0.2523244$	

Table A1. Values of the parameters of the EDIP potential for the case of silicon, obtained from fits to ab initio calculations based on Density Functional Theory (DFT).

The values of the potential are given in the following table

For Stillinger-Weber, we have

$$E_i = \sum_{j>i} \phi_2(r_{ij}) + \sum_{j \neq i} \sum_{k>j} \phi_3(r_{ij}, r_{ik}, \theta_{ijk}) \quad (\text{A.9})$$

where

$$\phi_2(r_{ij}) = A_{ij} \epsilon_{ij} \left[B_{ij} \left(\frac{\sigma_{ij}}{r_{ij}} \right)^{p_{ij}} - \left(\frac{\sigma_{ij}}{r_{ij}} \right)^{q_{ij}} \right] \exp \left(\frac{\sigma_{ij}}{r_{ij} - a_{ij} \sigma_{ij}} \right), \quad (\text{A.10})$$

$$\phi_3(r_{ij}, r_{ik}, \theta_{ijk}) = \lambda_{ijk} \epsilon_{ijk} [\cos(\theta_{ijk}) - \cos(\theta_{0ijk})]^2 \exp \left(\frac{\gamma_{ij} \sigma_{ij}}{r_{ij} - a_{ij} \sigma_{ij}} \right) \exp \left(\frac{\gamma_{ik} \sigma_{ik}}{r_{ik} - a_{ik} \sigma_{ik}} \right) \quad (\text{A.11})$$

The parameters used for silicon are

$A = 7.049556277$	$\lambda = 21.0$
$B = 0.6022245584$	$\gamma = 1.20$
$a = 1.80$	$\sigma = 0.20951$ nm
$p = 4$	$\epsilon = 3.4723 \times 10^{-12}$ erg/at
$q = 0$	

For the Tersoff potential,

$$E_i = \frac{1}{2} \sum_i \sum_{j \neq i} V_{ij} \quad (\text{A.12})$$

where

$$V_{ij} = f_C(r_{ij}) [f_R(r_{ij}) + b_{ij} f_A(r_{ij})], \quad (\text{A.13})$$

$$f_C(x) = \begin{cases} 1 & r < R - D \\ \frac{1}{2} - \frac{1}{2} \sin \left(\frac{\pi}{2} \frac{r-R}{D} \right) & R - D < r < R + D \\ 0 & r > R + D \end{cases}, \quad (\text{A.14})$$

$$f_R(r) = A \exp(-\lambda_1 r), \quad (\text{A.15})$$

$$f_A(r) = -B \exp(-\lambda_2 r), \quad (\text{A.16})$$

$$b_{ij} = (1 + \beta^n \varsigma_{ij}^n)^{-\frac{1}{2n}}, \quad (\text{A.17})$$

$$\varsigma_{ij} = \sum_{k \neq i,j} f_C(r_{ij}) g(\theta_{ijk}) \exp[\lambda_3^m (r_{ij} - r_{ik})^m] \quad (\text{A.18})$$

$$g(\theta) = \gamma_{ijk} \left(1 + \frac{c^2}{d^2} - \frac{c^2}{[d^2 + (\cos(\theta) - \cos(\theta_0))^2]} \right) \quad (\text{A.19})$$

Acknowledgements

G. Gutiérrez appreciates support from project PAIFAC-2016, Facultad de Ciencias, Universidad de Chile. F. González-Cataldo thanks support from CONICYT, postdoctoral scholarship Becas Chile 74160058.

References

- [1] Hu J Z, Merkle L D, Menoni C S and Spain I L 1986 *Phys. Rev. B* **34** 4679–4684
- [2] Mujica A, Rubio A, Muñoz A and Needs R J 2003 *Reviews of Modern Physics* **75** 863–912
- [3] Belonoshko A, Skorodumova N V, Rosengren A and Johansson B 2006 *Physical Review B* **73** 012201
- [4] Liu C M, Xu C, Cheng Y, Chen X R and Cai L C 2015 *Journal of Applied Physics* **118** 235901
- [5] Burakovsky L, Chen S P, Preston D L and Sheppard D G 2014 *Journal of Physics: Conference Series* **500** 162001
- [6] González-Cataldo F, Davis S and Gutiérrez G 2016 *Scientific Reports* **6** 26537
- [7] Li D, Zhang P and Yan J 2014 *Scientific reports* **4** 4707
- [8] Allen M P and Tildesley D J 1989 *Computer simulation of liquids* (Oxford university press)
- [9] Plimpton S 1995 *Journal of computational physics* **117** 1–19
- [10] Tersoff J 1989 *Phys. Rev. B* **39** 5566–5568
- [11] Tersoff J 1988 *Phys. Rev. B* **38** 9902–9905
- [12] Justo J a F, Bazant M Z, Kaxiras E, Bulatov V V and Yip S 1998 *Phys. Rev. B* **58** 2539–2550
- [13] Stillinger F H and Weber T A 1985 *Phys. Rev. B* **31** 5262–5271
- [14] Kumagai T, Izumi S, Hara S and Sakai S 2007 *Computational materials science* **39** 457–464
- [15] Li D, Zhang P, Yan J and Liu H Y 2011 *EPL (Europhysics Letters)* **95** 56004
- [16] Davis S, Belonoshko A, Johansson B, Skorodumova N V and van Duin A C T 2008 *The Journal of chemical physics* **129** 194508
- [17] Davis S, Loyola C, González F and Peralta J 2010 *Computer Physics Communications* **181** 2126–2139
- [18] Stukowski A 2009 *Modelling and Simulation in Materials Science and Engineering* **18** 015012
- [19] Deb S K, Wilding M, Somayazulu M and McMillan P F 2001 *Nature* **414** 528–530
- [20] Young D A 1991 *Phase Diagrams of the Elements* (University of California Press)
- [21] Zhang W J, Liu Z L and Peng Y F 2014 *Physica B: Condensed Matter* **449** 144–149